ISSN 0208-7774 TRIBOLOGIA 5/2018 p. 143–151

Agnieszka WIELOWIEJSKA-GIERTUGA[*], Tomasz WIŚNIEWSKI[**], Rafał RUBACH[**]

FRETTING CORROSION STUDIES OF MATERIALS USED FOR ELEMENTS OF HIP JOINT ENDOPROSTHESES

BADANIA FRETTING-KOROZJI MATERIAŁÓW STOSOWANYCH NA ELEMENTY ENDOPROTEZ STAWU BIODROWEGO

Key words: endoprosthesis, fretting, corrosion, wear, metal-on-metal articulation.

Abstract

The operational durability of a hip endoprosthesis depends, among others, on the intensity of the damage processes of kinematic junction elements caused by fretting corrosion processes. In the article, the results of comparative studies on the fretting corrosion resistance of alloys commonly used for hip joints, i.e. Ti6Al4V, CoCrMo, stainless steel M30NW, and 316LVM, are presented. The research was carried out by means of a tribological pin-on-disc tester working in reciprocating motion, integrated with a potentiostat equipped with a triac electrode. The tribosystem was a pin pressed by a constant force to a reciprocating disc with a certain amplitude and frequency. The tests were carried out in a medium of aqueous bovine serum heated to 37°C. The conducted comparative tests of the above mentioned materials will allow selection of the best material combination in terms of tribological and fretting corrosion resistance.
Under optimized conditions, the modified oils obtained a needed appropriate viscosity class.

Słowa kluczowe: endoproteza, fretting, korozja, zużycie, skojarzenie materiałowe metal-metal.

Streszczenie

Trwałość eksploatacyjna endoprotez stawu biodrowego zależna jest między innymi od intensywności procesów niszczenia elementów połączeń kinematycznych wywołanych procesami korozji frettingowej. W artykule przedstawiono wyniki porównawczych badań odporności na korozję frettingową stopów powszechnie stosowanych na elementy endoprotez stawu biodrowego: Ti6Al4V, CoCrMo, M30NW oraz 316LVM. Badania realizowano za pomocą testera tribologicznego typu pin-on-disc pracującego w ruchu posuwisto-zwrotnym, zintegrowanego z potencjostatem wyposażonym w układ trójelektrodowy. Skojarzenie badawcze stanowił trzpień dociskany ze stałą siłą do płytki poruszającej się ruchem posuwisto-zwrotnym o określonej amplitudzie i częstotliwości. Testy przeprowadzono w środowisku roztworu wodnego surowicy bydlęcej podgrzanej do temperatury 37°C. Przeprowadzone testy porównawcze wymienionych materiałów pozwolą na wytypowanie najkorzystniejszego skojarzenia materiałowego pod względem tribologicznym oraz odporności na fretting-korozję.

INTRODUCTION

Every year around the world about one million of hip replacement operations are performed. It is anticipated that the number of operations will increase due to the increase in longevity of the population. At the same time, the average age of people undergoing hip replacements is decreasing [**L. 1**]. It is therefore important to seek new materials that will prolong the life of the prosthesis and thus delay the need to carry out a revision operation. The occurrence of fretting corrosion in modular hip joint endoprostheses is a significant cause of decreased implant life and leads to the necessity to replace the implant [**L. 2**].

Modular endoprostheses are currently one of the most common types of hip joint endoprostheses. The most commonly used materials to produce hip implants are titanium, stainless steel, and CoCrMo alloys. These alloys are characterized by the ability of passivation, i.e. the formation of an oxide layer on them which protects against corrosion.

[*] Metal Forming Institute, ul. Jana Pawła II 14, 61-139 Poznań, Poland, tel.: +48 61 657 05 55, e-mail: agnieszka.wielowiejska-giertuga@inop.poznan.pl.
[**] Metal Forming Institute, ul. Jana Pawła II 14, 61-139 Poznań, Poland.

Fretting in hip joint endoprostheses occurs in the case of stationary junctions, which is the head-stem neck junction, in which the surfaces in direct contact perform movements with less amplitude than the width of the contact surface at that point [**L. 3**].

Fretting corrosion is defined as a wear process in which chemical and electrochemical reactions predominate. During the friction process, the surface of one element behaves like an anode and the surface of the other element as a cathode. At the moment of initiating movement, breaking of the oxide passivation layer on the alloy surface occurs. As a result of passivation layer damage, the surface reacts strongly with the oxygen-rich electrolyte present on the interfacial surface. Metal oxides rapidly and spontaneously reduce the oxygen contained in the liquid. As a consequence, the concentration of free metal ions on the interfacial surface increases. When the solubility of the cations is reached, further dissolution is due to the hydrolysis reaction. In the absence of OH- ions, Cl- ions migrate to the contact surface to compensate for the forming H+ ions and ensure neutrality of the electrolyte. As a result, the electrolyte is locally acidified, leading to accelerated corrosion [**L. 4**]. The factors influencing fretting corrosion are the following: load, contact area, frequency, the number of cycles, the extent of damage to the fretting zone, the number of trapped wear products between the contact surfaces, and corrosivity of the medium [**L. 5**]. Knowing and understanding the phenomenon of fretting corrosion present in orthopaedic materials will allow future materials to be prolonged to maximize the life of endoprostheses [**L. 6**].

One of the methods of testing and determining the material resistance to fretting corrosion is to conduct tribological tests in reciprocating motion using a potentiostat equipped with a triad electrode system. Within the present work, a number of tests were performed to compare and create a database of the resistance to fretting-corrosion of materials used to manufacture modular hip joint endoprostheses.

MATERIALS AND TEST METHODS

The fretting corrosion test stand consists of a T-17 Triband Tester (ITeE Radom) integrated with an SP-150 potentiostat (Bio-Logic Science Instruments). The tribosystem was a fixed pin pressed with a constant force of 100 N to a sample of dimensions Ø14×10 mm as the working electrode. As the current electrode, a platinum electrode was used, while the reference electrode was a saturated calomel electrode (SCE). **Fig. 1** shows a diagram of the tribosystem and a schematic diagram for the fretting corrosion test. To isolate the conductive elements of the tribosystem from the metal parts of the tester, a measuring cell made of Teflon was made and the pin was mounted in a special plastic casing. The tribosystem constituted the friction pairs shown in **Table 1**, selected on the basis of analysis of materials commonly used in arthroplasty.

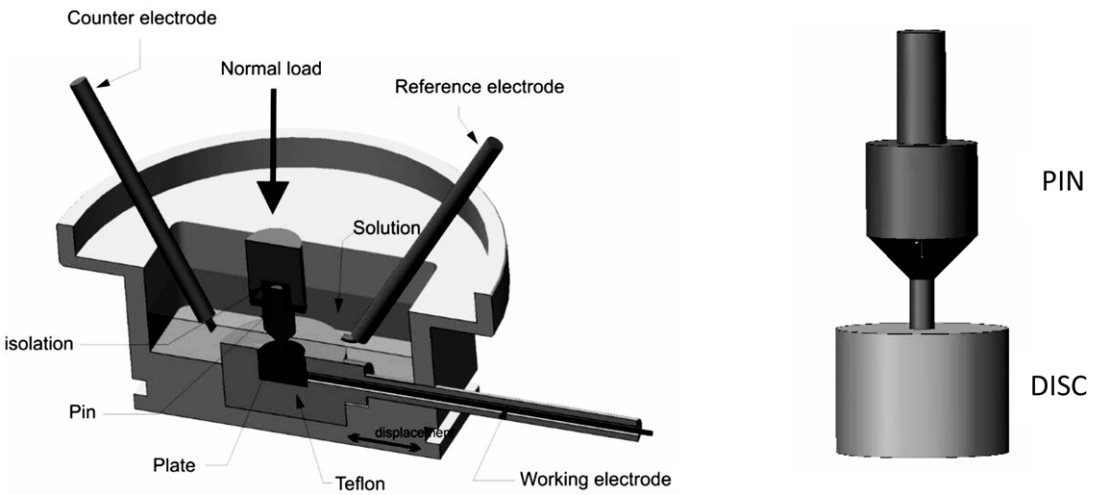

Fig. 1. Tribosystem (A) and diagram of fretting corrosion test system (Tribological Tester T-17 and SP-150 potentiostat)
Rys. 1. Skojarzenie badawcze (A) oraz schemat układu do badania fretting-korozji (tester tribologiczny T-17 i potencjostat SP-150)

The tests were carried out in reciprocating motion with a frequency of 1 Hz and a stroke length of 400 μm. The pin diameter at the contact point was 2 mm. The tests were performed in an aqueous solution of bovine serum prepared according to ISO 14242-1 [**L. 7**]. The bovine serum was diluted with deionized water to a protein content of 30 g/l ±2 g/l. In order to mask the calcium ions and minimize calcium phosphate precipitation on

the carrier surfaces that could significantly affect the coefficient of friction, ethylenediaminetetraacetic acid (EDTA) was added at the concentration of 20 mM (7.45 g/l) sodium azide in the concentration of 0.3% and as an antibacterial reagent. Before testing, the bovine serum solution was filtered through a sterile filter with a pore diameter of 2 μm to remove impurities.

Table 1. Metal-metal tribosystems
Tabela 1. Badane skojarzenia materiałowe typu metal–metal

Pin material	Sample material
CoCrMo	CoCrMo
	Ti6Al4V
	SS
Ti6Al4V	CoCrMo
	Ti6Al4V
	SS
SS	CoCrMo
	Ti6Al4V
	SS
SS 1.4441	SS 1.4441
SS – M30NW stainless steel SS 1.4441 – 316LVM stainless steel	

Before testing, the surfaces of the samples and counter specimens were ground to obtain an Ra roughness of 0.4 μm. This value corresponds to the quality of the metal surface of the head of the hip endoprosthesis in the head-stem neck modular junction. Before the test, the samples were washed in ethanol (10 min) and distilled water (10 min) using an ultrasonic cleaner and then thoroughly dried.

Each test was divided into three phases. The first, lasting 5400 s, is when the loaded sample is immersed in a static lubricating medium (no pin displacement with respect to the disc). The second is when the tribosystem is loaded and fretting is commenced. After another 3600 s, fretting is stopped and the tribosystem is unloaded. For each friction pair, 5 repetitions were performed.

On the basis of the obtained open circuit potential values during the whole test, the values of parameters such as the decrease in the open circuit potential value during fretting activation (Egap), the mean fretting potential value (Eavg), the potential change during fretting (ΔE), and the increase in open circuit potential during repatriation (Erec). These parameters are shown in **Fig. 2**.

The surface roughness measurements were carried out using a T8000 profilometer (Hommel) with a TKU300 measuring tip.

The following paper presents the results of reference materials implemented within the European collaborative project HypOrth: "New approaches in the development of implant material Hypoallergenic in Orthopedics: Steps to personalized medicine." The work is a continuation of the research presented in article [**L. 8**]. A further stage of work is expected to conduct comparative research of new materials for use in hip replacement.

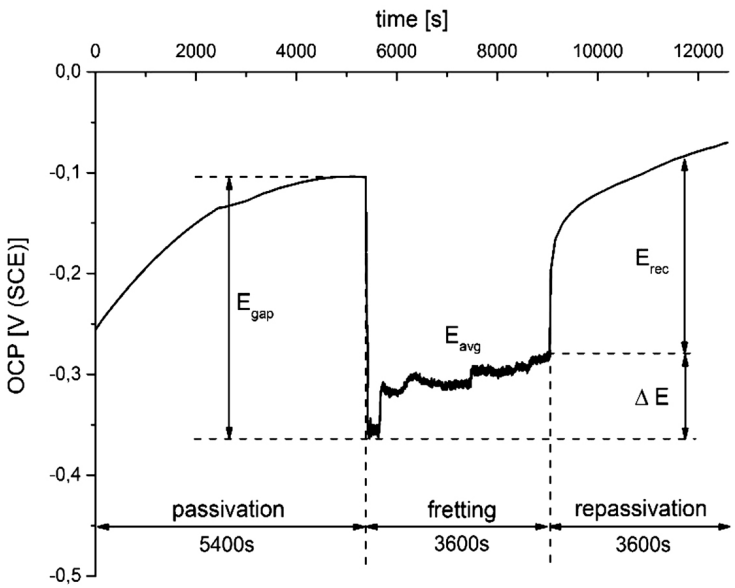

Fig. 2. Representation of criteria used to describe behaviour of potential throughout fretting experiment
Rys. 2. Przedstawienie kryteriów wykorzystanych do opisu zmian potencjału w trakcie frettingu

TEST RESULTS

Potentiodynamic studies

The graphs show the range of changes in the decrease in open circuit value (E_{gap}) during fretting activation (**Fig. 3**) and the mean values of the (E_{avg}) potential during fretting (**Fig. 4**) for the individual material combinations.

Both the open circuit potential value during activation and the mean value during fretting are dependent on the material of the friction pair. The smallest potential drop was observed for the SS (pin) – Ti6Al4V (disc) pair, while the largest was for the Ti6Al4V (pin) – Ti6Al4V (disc). The mean fretting potential values reached the lowest values for the SS (pin) – Ti6Al4V (disc) pair and Ti6Al4V (pin) – Ti6Al4V (disc) pair, while the highest was reached by the SS 1.4441 – SS 1.4441 pair.

Examining the sample potential in the open circuit allows initial assessment of the material resistance to corrosion. The effect of fretting on the potential changes is clearly shown in the graphs (**Fig. 5**), which show the course of open circuit potential (OCP) for individual friction pairs.

All the friction pairs showed a rise in anode voltage at the first stage of the test (before fretting was activated), suggesting a thickening of the passive protective layer. After 90 minutes of potential stabilization, the fretting friction process was started, which led to destruction of the protective oxide layer. A sharp decrease in the corrosive potential value occurred. In the first phase of fretting, the potential decrease was significant for several friction pairs and then settled at a certain value (CoCrMo – SS, CoCrMo – Ti6Al4V, Ti6Al4V – Ti6Al4V, SS – CoCrMo, SS – Ti6Al4V), suggesting

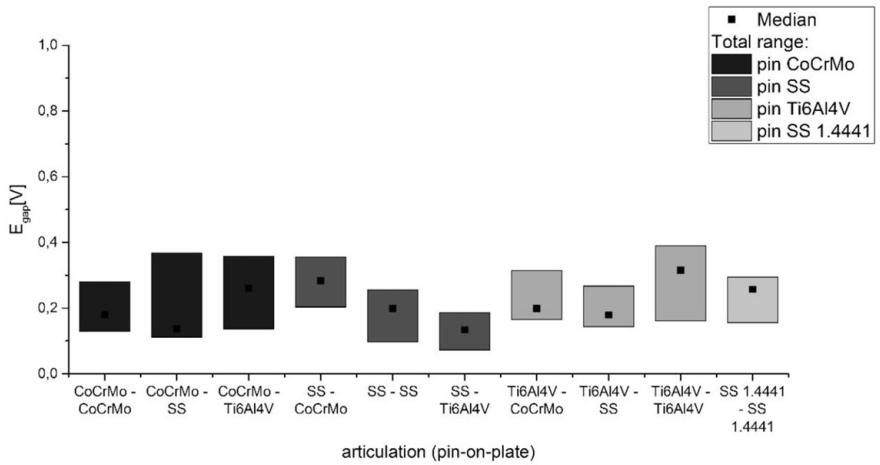

Fig. 3. Change in open circuit potential value Egap for tested material combinations
Rys. 3. Zmiana wartości potencjału obwodu otwartego Egap dla badanych skojarzeń materiałowych

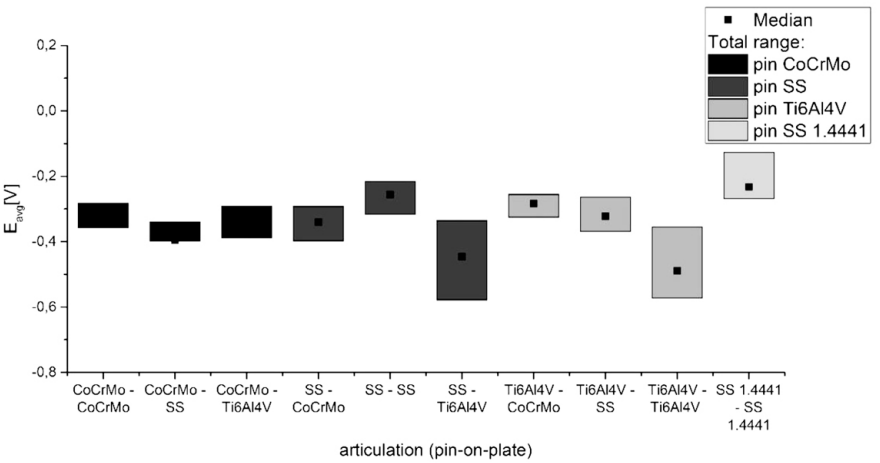

Fig. 4. Mean value of open circuit potential Eavg during fretting for tested material combinations
Rys. 4. Średnia wartość potencjału obwodu otwartego Eavg w trakcie trwania frettingu dla badanych skojarzeń materiałowych

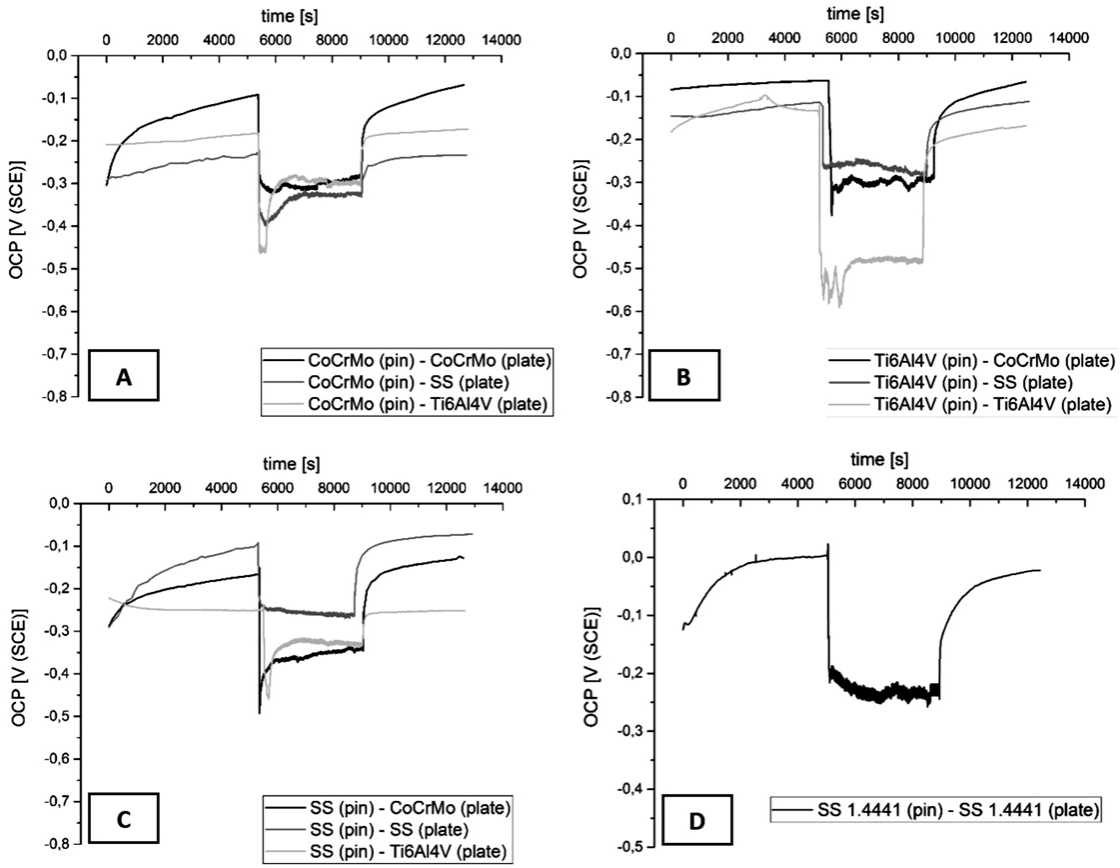

Fig. 5. Course of changes in open circuit potential during whole test: A – CoCrMo pin; B – Ti6Al4V pin; C – SS pin; D – SS 1.4441 pin

Rys. 5. Przebieg zmian potencjału obwodu otwartego w trakcie trwania całego testu: A – pin CoCrMo; B – pin Ti6Al4V; C – pin SS; D – pin SS 1.4441

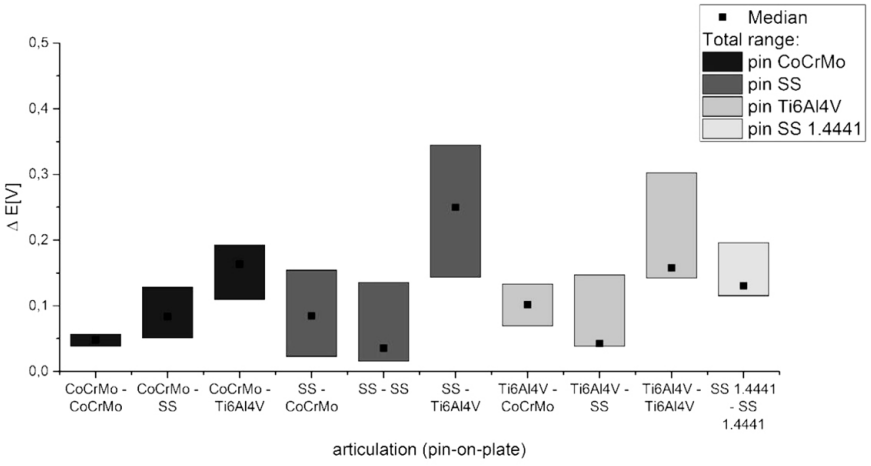

Fig. 6. Range of changes in open circuit potential value ΔE during fretting for tested material combinations

Rys. 6. Zakres zmian wartości potencjału obwodu otwartego ΔE w trakcie frettingu dla badanych skojarzeń materiałowych

significant depolarization during fretting activation for the other pairs. Fluctuations in the open circuit potential values (OCP) during fretting indicate alternating depolarization and repatriation. At this stage, the value of the potential settled at a constant value, which is caused by the occurrence of a balance between the processes of

passivation and depassivation during fretting. For some material pairs (Ti6Al4V – SS, SS – CoCrMo, SS1.4441 – SS 1.4441), the course of potential changes during fretting was decreasing, which indicates predominance of the depassivation process over repatriation. After 60 minutes from friction activation, the oxide layer is rebuilt and the potential rises to the pre-fretting value. The destroyed oxide layer is not completely rebuilt in some cases. This is particularly evident for the friction pairs where both the disc and the pin constituted the Ti6Al4V alloy, as well as the SS 1.4441 (pin) – SS 1.4441 (disc), which was also noted by the authors of [**L. 9**] in their research. This is demonstrated by lower values of open circuit potential at the end of the test (after repatriation) than after the first test phase (passivation). It is obvious that mechanical and electrochemical oxide interactions depend on the chemical composition and structure of the oxides on the surface and their interaction. In order to clarify the mechanisms involved during fretting corrosion, further research is required.

The range of changes in the open circuit potential value (ΔE) during fretting (**Fig. 6**) differs for individual material combinations. The smallest values were for the CoCRMo (pin) – CoCrMo (disc), Ti6Al4V (pin) – SS (disc) and SS (pin) – SS (disc) pairs, which indicates slight fluctuations in the open circuit potential during fretting and characterized then by on-going depassivation and repassivation processes as stable.

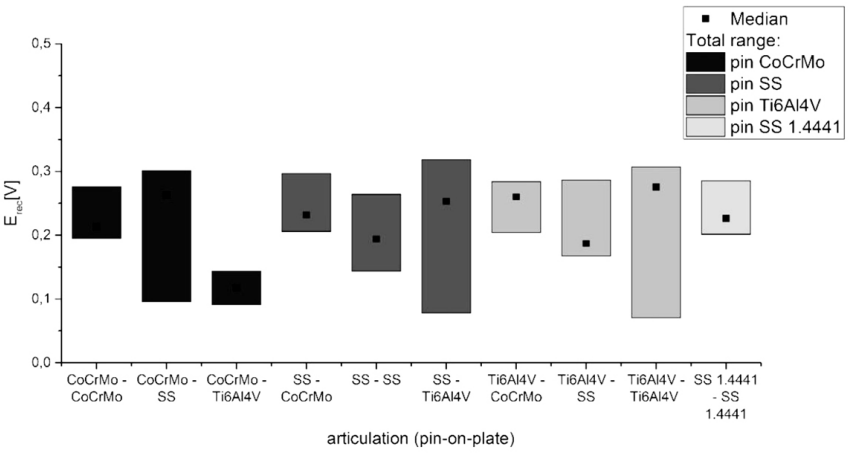

Fig. 7. Change in open circuit potential value Erec after turning off fretting for tested material combinations
Rys. 7. Zmiana wartości potencjału obwodu otwartego Erec po wyłączeniu frettingu dla badanych skojarzeń materiałowych

Table 2. Summary of median values for parameters describing fretting corrosion process
Tabela 2. Zestawienie wartości mediany dla parametrów opisujących proces fretting-korozji

Material combination	E_{gap}	E_{avg}	ΔE	E_{rec}
CoCrMo(pin) – CoCrMo(disc)	0.18005	–0.3071	0.0478	0.2132
CoCrMo(pin) – SS(disc)	0.13755	–0.3961	0.0838	0.2629
CoCrMo(pin) – Ti6Al4V(disc)	0.26097	–0.3182	0.1632	0.1172
SS(pin) – CoCrMo(disc)	0.28309	–0.3400	0.0847	0.2316
SS(pin) – SS(disc)	0.19889	–0.2560	0.0357	0.1939
SS(pin) – Ti6Al4V(disc)	0.13381	–0.4462	0.2499	0.2529
Ti6Al4V(pin) – CoCrMo(disc)	0.19855	–0.2839	0.1015	0.2598
Ti6Al4V(pin) – SS(disc)	0.17899	–0.3217	0.04263	0.1869
Ti6Al4V(pin) – Ti6Al4V(disc)	0.31539	–0.4896	0.1576	0.2754
SS 1.4441 (pin) – SS 1.4441(disc)	0.25677	–0.2328	0.13061	0.2259

The potential values during the various stages of the test are presented in the **Table 2**.

Repassivation rate

The repassivation rate was also determined to compare tested combinations of materials and their ability to rebuild the protective passive layer. This is an OCP

proportionality indicator 30 seconds after stopping fretting process against the OCP measured after 1 hour after the passive film has been removed.

The lowest repassivation rate was found for material combinations where the disc was made of stainless steel (12.2–15,6%), while the highest values were obtained for discs made of Ti6Al4V (44.9–48,5%). Discs made of CoCrMo alloy exhibited a repassivation rate similar to that of titanium alloy and ranged from 40.4 to 44.8%. The values obtained are similar to the values obtained by the authors of article [**L. 10**]. The higher repassivation rate for SS 316LVM stainless steel (SS 1.4441) compared to M30NW stainless steel is confirmed by the authors of article [**L. 11**]. Differences in the repassivation rate

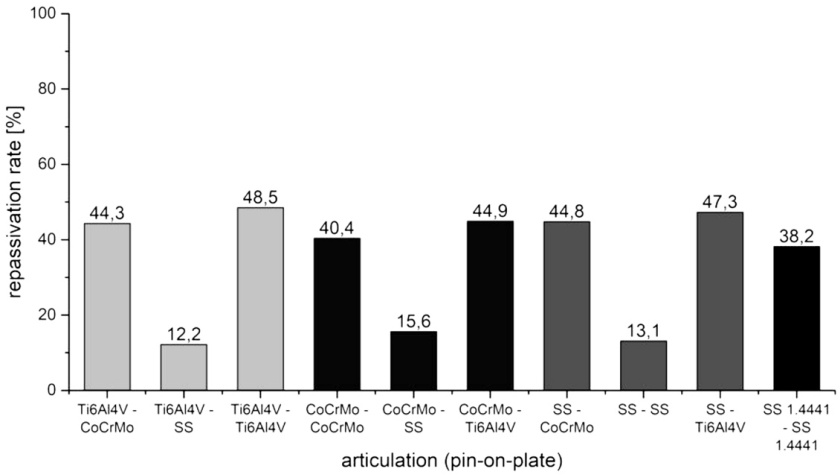

Fig. 8. Repassivation rate of tested material combinations
Rys. 8. Wskaźnik repasywacji dla danych skojarzeń materiałowych

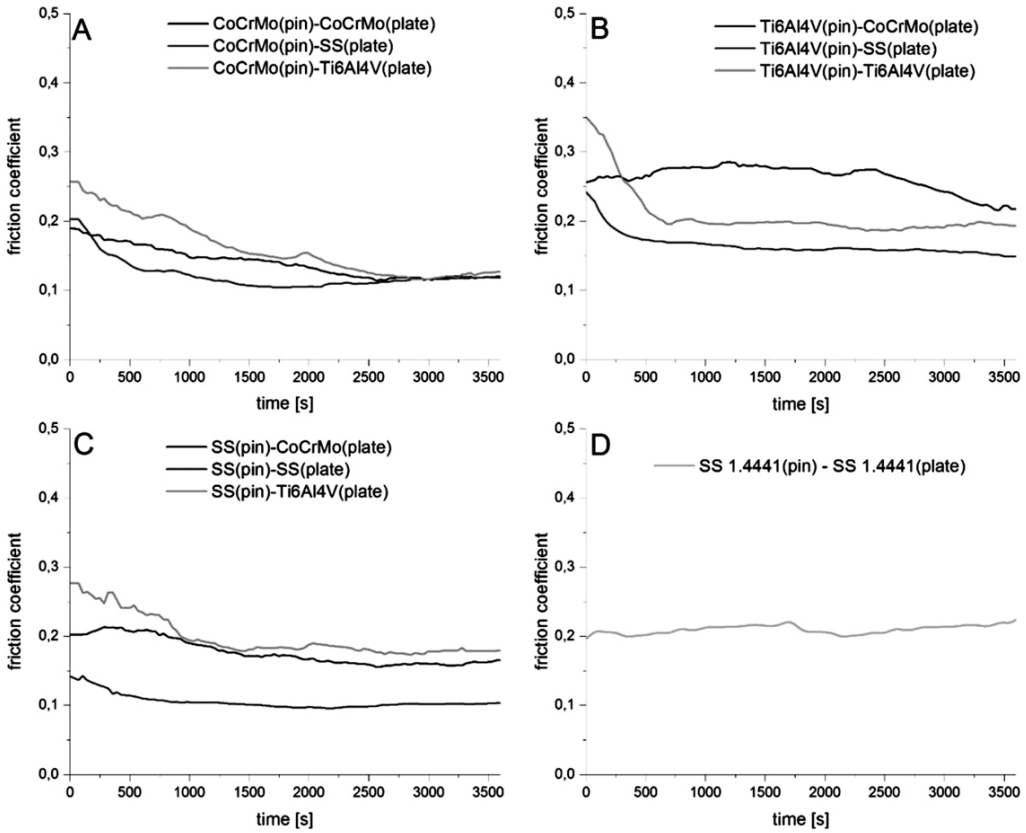

Fig. 9. Changes of friction coefficient during fretting: A – pin CoCrMo; B – SS pin; C – pin Ti6Al4V; D – pin SS 1.4441
Rys. 9. Przebieg zmian współczynnika tarcia w trakcie frettingu: A – pin CoCrMo; B – pin SS; C – pin Ti6Al4V; D – pin SS 1.4441

for each material depend on the electrochemical and chemical reactions in the environment of a solution of bovine serum under fretting-corrosion. Better understanding of these processes requires additional testing and will be the subject of further research.

Coefficient of friction

For all the friction pairs, except SS 1.4441 – SS 1.4441, a decrease in the friction coefficient was observed (**Fig. 8**). The coefficients of friction and their course were different for each friction pair. The smallest mean values (μ = 0.105) were recorded for the SS (pin) – SS (disc) pair, while the largest (μ = 0.263) was for the Ti6Al4V (pin) – CoCrMo (disc) pair. The average values of friction coefficient are presented in **Table 3**. There was no correlation between the open circuit potential during fretting and the friction coefficient values.

Table 3. Comparison of mean coefficient of friction for individual material combinations
Tabela 3. Zestawienie średniego współczynnika tarcia dla poszczególnych skojarzeń materiałowych

Material combination (pin-on-disc)	Mean coefficient of friction
CoCrMo(pin) – CoCrMo(disc)	0.140
CoCrMo(pin) – SS(disc)	0.122
CoCrMo(pin) – Ti6Al4V(disc)	0.161
SS(pin) – CoCrMo(disc)	0.177
SS(pin) – SS(disc)	0.105
SS(pin) – Ti6Al4V(disc)	0.197
Ti6Al4V(pin) – CoCrMo(disc)	0.263
Ti6Al4V(pin) – SS(disc)	0.165
Ti6Al4V(pin) – Ti6Al4V(disc)	0.207
SS 1.4441 (pin) – SS 1.4441(disc)	0.210

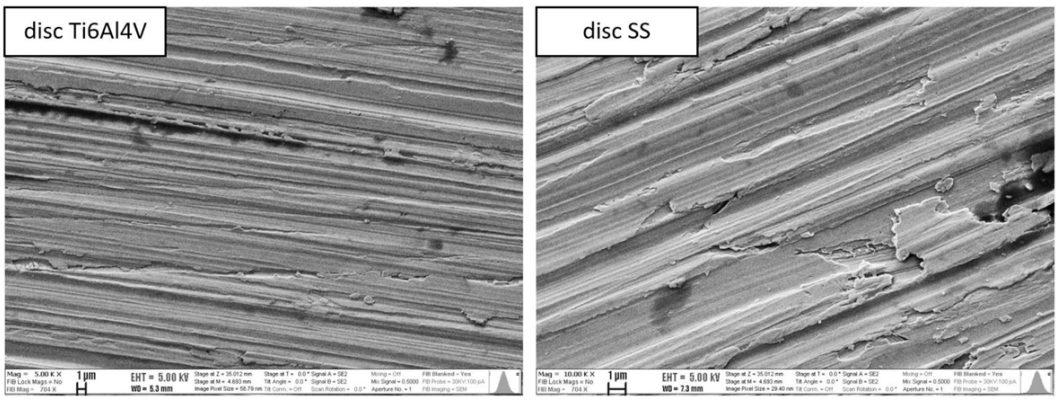

Fig. 10. Surface morphology of samples after fretting-corrosion tests
Rys. 10. Morfologia powierzchni próbek po testach fretting-korozji

After corrosion and fretting corrosion tests, all samples were characterized by SEM and EDS to define a corrosion morphology (**Fig. 10**).

The microscopic observation of the surface is clear information that an intensive process of fretting wear has occurred. Poor removal of wear products from the friction zone is characteristic of the fretting process, and a high wear debris concentration is observed at the edges of the wear area.

CONCLUSIONS

Based on the conducted analysis, the following conclusions were made:

1. The best resistance to fretting corrosion in bovine serum is shown by the SS (pin) – Ti6Al4V (disc) pair (lowest Egap).
2. During fretting, the lowest mean values of open circuit potential were recorded for the SS (pin) – Ti6Al4V (disc) and Ti6Al4V – Ti6Al4V pairs.
3. After the fretting process has been completed, the repatriation process for most pairs is complete. Exceptions are the pairs made of Ti6Al4V – Ti6Al4V alloy and SS 1.4441 – SS 1.4441.
4. The lowest values of friction coefficient were exhibited by the pairs working in the SS-SS system, while the highest values were recorded for the Ti6Al4V – CoCrMo friction pair. The course of the coefficient of friction for the SS 1.444 – SS 1.4441 pair was characterized by an upward trend, while, for the remaining pairs, the coefficient of friction decreased during the test.

The research results show that the highest resistance to fretting corrosion is characterized by the SS (pin) – Ti6Al4V (disc).

ACKNOWLEDGEMENTS

The research leading to these results received funding from the European Union Seventh Framework Programme FP7/2007–2013 under grant agreement No. 602398.

The research work was financed from public funds for Science in the period 2013–2018, granted for realization of an international co-financed project.

REFERENCES

1. Holzwarth U., Cotogno G.: Total hip arthroplasty: State of the art, challenges and prospects, Publications Office, Luxembourg 2012.
2. John Cooper H., et al.: Corrosion at the Head-Neck Taper as a Cause for Adverse Local Tissue Reactions After Total Hip Arthroplasty, The Journal of Bone and Joint Surgery-American Volume vol. 94 (2012), s. 1655–1661.
3. Geringer J., Macdonald D.D.: Friction/fretting-corrosion mechanisms: Current trends and outlooks for implants, Materials Letters vol. 134 (2014), s. 152–157.
4. Tritschler B., Forest B., Rieu J.: Fretting corrosion of materials for orthopaedic implants: a study of a metal/polymer contact in an artificial physiological medium, Tribology International vol. 32 (1999), s. 587–596.
5. Yan Y., Neville A., Dowson D.: Tribo-corrosion properties of cobalt-based medical implant alloys in simulated biological environments, Wear vol. 263 (2007), s. 1105–1111.
6. Rituerto Sin J., et al.: Fretting corrosion of hafnium in simulated body fluids, Tribology International vol. 75 (2014), s. 10–15.
7. (ISO 14242-1:2012) Implants for surgery – Wear of total hip-joint prostheses -- Part 1: Loading and displacement parameters for wear-testing machines and corresponding environmental conditions for test.
8. Sulej-Chojnacka J., et al.: Fretting corrosion of cobalt and titanium implant alloys in simulated body fluids., TRIBOLOGIA (2016), s. 149–158.
9. Bryant M. et al.: The role of surface pre-treatment on the microstructure, corrosion and fretting corrosion of cemented femoral stems, Biotribology vol. 5 (2016), s. 1–15.
10. Contu F., Elsener B., Böhni H.: Corrosion behaviour of CoCrMo implant alloy during fretting in bovine serum, Corrosion Science vol. 47 (2005), s. 1863–1875.
11. Park C.-J., Kwon H.-S.: Comparison of repassivation kinetics of stainless steels in chloride solution, Metals and Materials International vol. 11 (2005), s. 309–312.